Effect of Pulse Averaging on Sonic Anemometer Spectra

KATJA HENJES, PETER K. TAYLOR, AND MARGARET J. YELLAND

James Rennell Division, Southampton Oceanography Centre, Southampton, United Kingdom

14 August 1997 and 23 March 1998

ABSTRACT

Recent analysis of high quality Solent sonic anemometer spectra revealed a frequency-dependent systematic underestimation of the spectral levels with a minimum at about three-quarters of the Nyquist frequency. It is shown that this is due to the eightfold pulse average with which the Solent sonic achieves its nominal sampling frequency of 21 Hz, combined with the effects of aliasing. An explicit correction curve is developed.

1. Observation: Frequency dependence of spectral levels

The Solent sonic anemometer (Gill Instruments, Ltd.) is used increasingly for wind stress determination employing the inertial dissipation technique (Dupuis et al. 1995; Yelland and Taylor 1996; Yelland et al. 1998). In this paper we will examine the major set of high-frequency wind speed data that were obtained in 1993 on board the RRS *Discovery* during three cruises in the Southern Ocean. The anemometer samples the three components of the wind at a rate of 168 Hz, and the data are averaged to produce the nominal sampling frequency of 21 Hz output by the instrument. The asymmetric head version of the Solent sonic was used, with the 240° open section facing the bow of the ship. The data were quality controlled for minimized flow distortion (only wind directions within $\pm 10°$ of the bow were accepted), absence of ship maneuvers, and steadiness of mean wind direction (Yelland et al. 1998). The data were then processed with a fast Fourier transform routine to obtain spectra. The spectral levels estimated between 2 and 4 Hz could be related to the dissipation rate of the turbulent kinetic energy (TKE) by Kolmogorov's universal relation, and finally, the wind stress was calculated from the dissipation rate via the TKE budget (Yelland and Taylor 1996).

The same data were studied again recently to investigate systematically how to optimize the processing strategy (Henjes 1997). Very well-defined spectra were obtained by evaluating a total of 359 12-min runs spanning a 10-week period from February to the end of April 1993. The individual spectra had satisfied the $f^{-5/3}$ criteria in the 2–4-Hz range, as required by Yelland and Taylor (1996). A significant systematic departure from a $f^{-5/3}$ slope was found, however, when the averaged spectra were examined at frequencies above 4 Hz. This is shown in Fig. 1, which depicts the averaged power spectral density, flattened by multiplication with $f^{5/3}$. The along-wind, crosswind, and vertical components are defined by the sample mean wind. The individual spectra were summed unnormalized and thus were obtained without the need to determine the friction velocity u_* first. This overemphasizes the high-wind behavior, and the average is dominated by the spectra obtained at wind speeds between 10 and 15 m s^{-1} but allows the frequency dependence of interest here to be easily studied.

The values below about 1 Hz are strongly influenced by the motion of the ship and cannot be expected to follow a universal behavior. There are also resonances mainly in the along-wind component at 5, 9, and, possibly, 7 Hz; these are likely to be due to vibrations of the sensor support structures. The residual spectral levels, however, fail to be frequency independent: the values at around 7–8 Hz are about 20% lower than those at 2–3 Hz.

The downslope cannot be explained by the well-known effect of path averaging (Kaimal et al. 1968) since it is clearly visible in spectra obtained at wind speeds greater than 20 m s^{-1}. At such wind speeds, and for the short pathlength ($L \approx 0.1$ m) of our instrument, path averaging would not be significant at frequencies lower than about 30 Hz since the effect of path averaging is significant only for $L2\pi f/U > 1$.

Although one would expect path averaging to be noticeable at lower wind speeds, in our data it is difficult to isolate different sources of scatter when averaging over smaller subsets of the data. Within the noise levels

Corresponding author address: Dr. Peter K. Taylor, James Rennell Centre for Ocean Circulation, Southampton Oceanography Centre, Room 254/27, European Way, Southampton SO14 3ZH, United Kingdom.
E-mail: P.K.Taylor@soc.soton.ac.uk

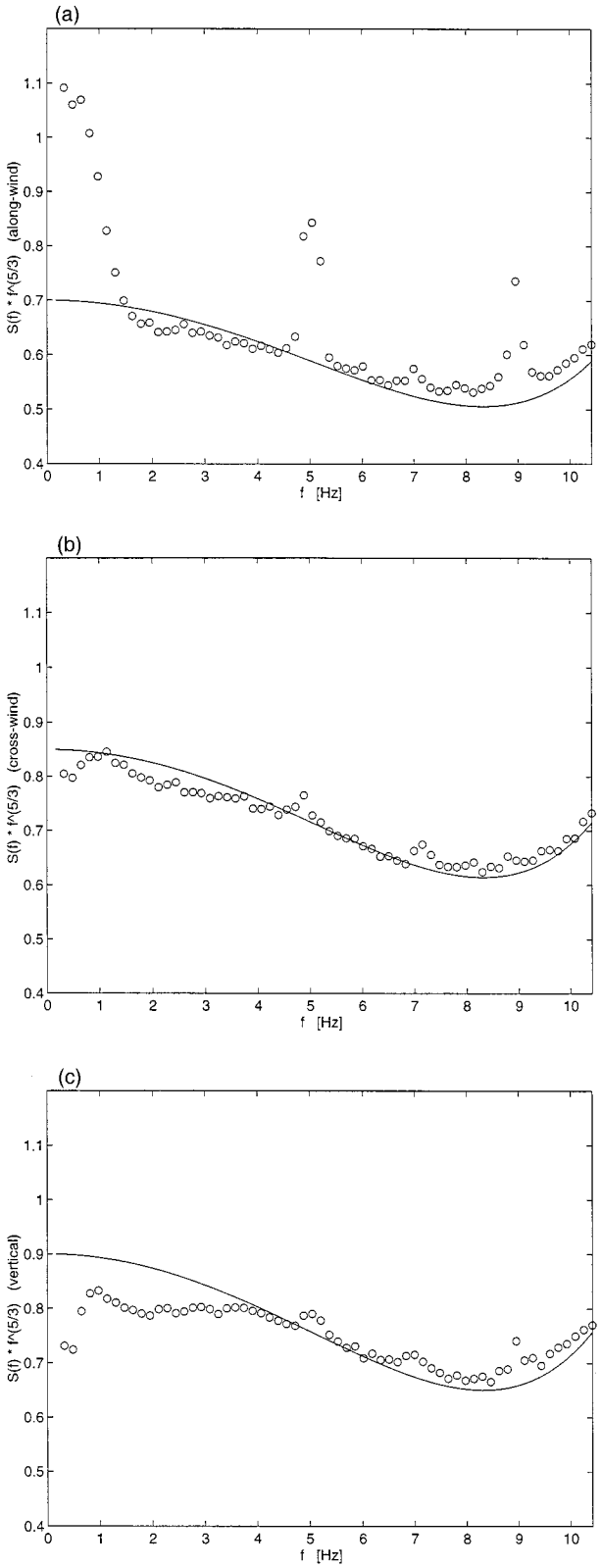

FIG. 1. Observed (a) along-wind, (b) cross-wind, and (c) vertical components of the power spectral density, multiplied by $10 f^{5/3}$, as functions of frequency. Sample wind coordinates are used. The spectra are unnormalized averages over a wide wind speed range; they present, the shape of the flattened spectra was found to be independent of mean wind speed U. This strongly points toward the sensor rather than the probed airflow giving rise to the effect, with the spectral variation depending on measured frequency rather than on natural wavenumber. In contrast, based on the frozen turbulence hypothesis, one would expect turbulent statistical properties of the airflow to scale with $U^{2/3}$, which is a variation that would have been clearly discernible.

In a previous study with a prototype Solent sonic, the spectral levels in the 0.8–2-Hz range had been found to be similar to those recorded with other types of anemometers (Yelland et al. 1994). These findings suggest that the frequency dependence arises from excess attenuation at higher frequencies rather than excess power at lower ones. In the following section it is shown that excess damping of higher frequencies is caused by the eightfold pulse average with which the Solent sonic achieves its nominal sampling frequency of 21 Hz. A similar mechanism was described by Larsen et al. (1993) in their analysis of temperature spectra measured with a Kaijo–Denki sonic anemometer. In that case, it was only one of a number of corrections found to be important.

2. Pulse average: Analytical correction formula

The Solent sonic delivers wind speed measurements at a sampling frequency of 21 Hz. This is achieved by block averaging eight data points measured at a rate of 168 Hz. Let us consider a time series of N wind speed measurements obtained at 21 Hz:

$$u_j^{\text{bloc}} = u^{\text{bloc}}(t = j\Delta t), \tag{1}$$

where $\Delta t = 1/21$ s and j runs from 0 to $N - 1$. The N values of u^{bloc} are block averages of eight points each obtained at 168 Hz:

$$u_k^{\text{sample}} = u^{\text{sample}}\left(t = k\frac{\Delta t}{8}\right), \tag{2}$$

where k runs from 0 to $8N - 1$. Then

$$u_j^{\text{bloc}} = \frac{1}{8}\sum_{k=8j}^{8j+7} u^{\text{sample}}\left(k\frac{\Delta t}{8}\right). \tag{3}$$

We then find for the Fourier transforms $\tilde{u}(f)$ (cf. the appendix):

$$\tilde{u}_n^{\text{bloc}} = \tilde{u}_n^{\text{bloc}}[f = n/(N\Delta t)] = \frac{1}{8}\sum_{s=0}^{7} \tilde{u}_{(n+sN)}^{\text{sample}} \frac{(e^{-i2\pi n/N} - 1)}{(e^{-i2\pi(n+sN)/8N} - 1)}. \tag{4}$$

Finally, the power spectral density $S(f)$ is found from

←

overemphasize the high wind behavior. The solid lines show the correction curve of Eq. (5).

the absolute square of $\tilde{u}$. As spectral estimates at different frequencies are statistically independent, on average, the spectrum is given as a sum of squares:

$$S(f_n) = \frac{1}{8^2}\sum_{s=0}^{7} S(f_{n+sN})\left|\frac{(e^{-i2\pi n/N} - 1)}{(e^{-i2\pi(n+sN)/8N} - 1)}\right|^2. \quad (5)$$

Equation (5) can be approximated by two straightforward contributions.

1) For small n (low frequencies), the exponentials can be expanded, resulting in a correction factor of $\sin^2(n\pi/N)/(n\pi/N)^2$ for $S(f_n)$—clearly the Fourier transform of the square hat window that represents the block average in the time domain. This is what might have been expected.

2) The true spectral densities decay rapidly with increasing frequency, following the $f^{-5/3}$ slope. Thus, only the lowest frequencies—that is, the $s = 0$ term—would contribute in Eq. (5). Dealing with discrete series, however, the terms $s = 4$–7 of $S(f_{n+sN})$ are mirror images of the $s = 0$–3 terms, with $s = 7$ being again a dominant contribution. These spurious high-frequency values add to the low-frequency spectral levels due to aliasing.

Assuming the $f^{-5/3}$ slope for the undisturbed spectrum, these two main attenuation factors can be written as functions of frequency f as

$$\text{att1}(f) = \left[\frac{\sin(\pi f \Delta t)}{\pi f \Delta t}\right]^2 \quad (6)$$

$$\text{att2}(f) = \left(\frac{f}{f_0 - f}\right)^{5/3}\left\{\frac{\sin[\pi(f_0 - f)\Delta t]}{\pi(f_0 - f)\Delta t}\right\}^2, \quad (7)$$

where f_0 is the nominal sampling frequency (here 21 Hz). As given in Eqs. (6) and (7), the factors modify the flattened spectral densities

$$[f^{5/3}S(f)]^{\text{sonic}} = [f^{5/3}S(f)]^{\text{true}}[\text{att1}(f) + \text{att2}(f)]. \quad (8)$$

To correct for the pulse-averaging loss, the measured spectra as obtained from the anemometer readings have to be divided by $[\text{att1}(f) + \text{att2}(f)]$.

The results of the theoretical analysis are shown in Fig. 2. The exact formula, Eq. (5), is displayed as circles (topmost curve). The star symbols represent the first-order effect of block averaging, the $\sin^2(\pi f\Delta t)/(\pi f\Delta t)^2$ decay of Eq. (6) (downward-sloping curve). The plus symbols depict the aliasing of this same curve, Eq. (7). The ''×'' symbols show the sum of the last two. They closely match the exact formula, indicating that the essence of the effect is well understood and that its main contributions are captured in two simple terms.

The exact formula [i.e., including all terms in the aliasing sum of Eq. (5)] is compared with the observed frequency dependence in Fig. 1 (solid lines). The agreement is very good. The overall shape of the frequency dependence and the position of the minimum are correct. The analytical formula seems to slightly overestimate

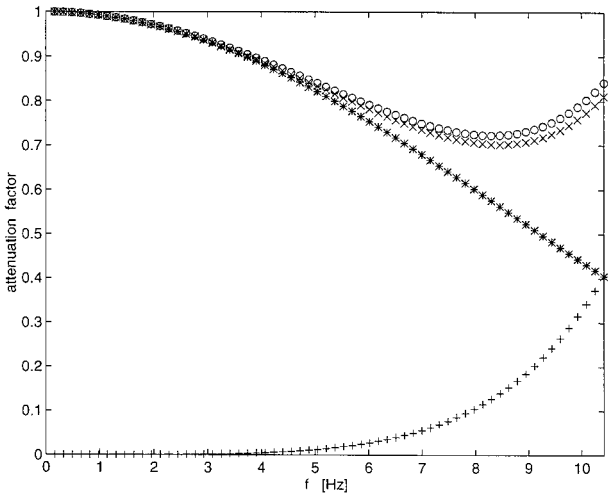

FIG. 2. Result of the theoretical analysis: exact formula of Eq. (5), ○; first-order effect of block averaging, Eq. (6), *; aliasing of block averaging, Eq. (7), +; and sum of first-order block average and its alias $[\text{att1}(f) + \text{att2}(f)]$, ×.

the waviness of the flattened spectral levels, especially in the vertical component. On the other hand, for the vertical spectrum, the low-frequency end of the inertial range may have been reached; $S_w(f)$ is known to level off at higher frequencies than the other two components (Kaimal et al. 1972).

From Eq. (5) the attenuation due to pulse averaging can be estimated for the flattened spectra, $f^{5/3}S(f)$, being 3% on average in a 1–3-Hz frequency range and 6% on average in a 2–4-Hz range. The maximum value in a 7–9-Hz range amounts to about 27%. The prototype Solent sonic tested by Yelland et al. (1994) used an average of two pulses only, causing an underestimation of the spectral levels of only 1% in the studied range of 0.8–2 Hz. These errors would cause biases of a slightly smaller magnitude in the calculated friction velocity; for example, an underestimate of 5% in the spectral level would cause a 3% underestimation of the friction velocity.

If a path-averaging term was included in the analysis, it would have little effect at low frequencies and would become significant for the higher frequencies only at wind speeds below 10 m s^{-1}. The effect of path averaging can be approximated by including the factor $\sin^2(\pi fL/U)/(\pi fL/U)^2$ in Eq. (5). This modifies the attenuation terms in the square brackets of Eq. (8) to

$$\left\{\frac{\sin^2(\pi fL/U)}{(\pi fL/U)^2}\text{att1}(f) + \frac{\sin^2[\pi(f_0 - f)L/U]}{[\pi(f_0 - f)L/U]^2}\text{att2}(f)\right\}. \quad (9)$$

The limited effect of this term is illustrated in Fig. 3. For wind speeds greater than 10 m s^{-1}, the modified attenuation term of Eq. (9) rapidly asymptotes to that given in Eq. (8).

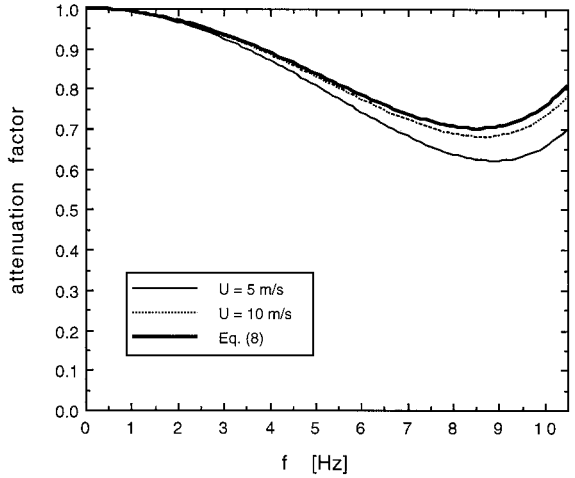

FIG. 3. The attenuation term [att1(f) + att2(f)] of Eq. (8) is illustrated by the thick solid line. The thin lines indicate the modification of this term by the inclusion of a path-averaging approximation as given in Eq. (9). The solid line indicates the modified attenuation for a wind speed of 5 m s^{-1}, and the dashed line shows the modified attenuation for a wind speed of 10 m s^{-1}. For wind speeds greater than 10 m s^{-1}, the attenuation term of Eq. (9) rapidly asymptotes to that of Eq. (8).

3. Conclusions

A frequency dependence has been observed in the ''flattened'' spectral levels $f^{5/3}S(f)$. It was visible in spectra obtained at wind speeds greater than 20 m s^{-1}, ruling out path averaging as a possible explanation. The effect was difficult to isolate from other sources of scatter when averaging over less than the whole dataset, and a systematic dependence on wind speed could not be studied. The $U^{2/3}$ dependence, as required by similarity theory if wavenumber rather than frequency were the crucial variable, was not observed. Hence, it is concluded that the effect is caused by the measuring anemometer and not the measured turbulent airflow. It is shown that the frequency dependence introduced by the eight-point block average, with which the Solent sonic anemometer achieves its nominal sampling frequency of 21 Hz, matches very well the shape of the observed spectral levels, indicating that the correct mechanism has been identified. The main contributions are shown to be the Fourier image of the eight-point square window and its alias.

An explicit correction curve is given. In the 2–4-Hz frequency range, for a nominal sampling frequency of 21 Hz, the attenuation amounts to about 6%. The damping is higher at higher frequencies. As higher frequencies might be required at lower heights, to ensure that measurements take place in the inertial subrange, the effect might be more disruptive for buoy-borne than shipborne observations.

Acknowledgments. This work was funded by the CEC as part of the EEC training project Air–Sea Fluxes. We are grateful for the helpful comments made by the brilliant anonymous reviewers.

APPENDIX

Fourier Transform for Block-Averaged Data

Definition of the Fourier transform:

$$\tilde{u}_n^{\text{bloc}} = \frac{1}{N}\sum_{l=0}^{N-1} u_l^{\text{bloc}} e^{i2\pi nl/N}. \tag{A1}$$

Here n takes on the values between 0 and $N - 1$. Insertion of Eq. (3):

$$\tilde{u}_n^{\text{bloc}} = \frac{1}{N}\sum_{l=0}^{N-1}\frac{1}{8}\sum_{r=0}^{7} u_{(8l+r)}^{\text{sample}} e^{i2\pi nl/N}. \tag{A2}$$

Write u^{sample} as a sum of $8N$ Fourier components:

$$\tilde{u}_n^{\text{bloc}} = \frac{1}{N}\sum_{l=0}^{N-1}\frac{1}{8}\sum_{r=0}^{7}\sum_{k=0}^{8N-1} \tilde{u}_k^{\text{sample}} e^{-i2\pi k(8l+r)/(8N)} e^{i2\pi nl/N}. \tag{A3}$$

Evaluation of the sum over I:

$$\tilde{u}_n^{\text{bloc}} = \frac{1}{8N}\sum_{r=0}^{7}\sum_{k=0}^{8N-1} \tilde{u}_k^{\text{sample}}\, e^{-i2\pi kr/(8N)} N\delta_{n,(k-sN)}. \tag{A4}$$

Here s is introduced as an arbitrary integer. As n runs to $N - 1$ but k to $8N - 1$, values of s from 0 to 7 will yield nonzero contributions to a sum over the Kronecker delta symbol. Put $j = k - sN$ and evaluate the sum over j:

$$\tilde{u}_n^{\text{bloc}} = \frac{1}{8}\sum_{s=0}^{7} \tilde{u}_{(n+sN)}^{\text{sample}} \sum_{r=0}^{7} e^{-i2\pi(n+sN)r/8N}. \tag{A5}$$

Evaluation of the sum over r (geometric series) yields Eq. (4):

$$\tilde{u}_n^{\text{bloc}} = \frac{1}{8}\sum_{s=0}^{7} \tilde{u}_{(n+sN)}^{\text{sample}} \frac{(e^{-i2\pi n/N} - 1)}{[e^{-i2\pi(n+sN)/8N} - 1]}. \tag{A6}$$

REFERENCES

Dupuis, H., A. Weill, K. Katsaros, and P. K. Taylor, 1995: Turbulent heat fluxes by profile and inertial dissipation methods: Analysis of the atmospheric surface layer from shipboard measurements during the SOFIA/ASTEX and SEMAPHORE experiments. *Ann. Geophys.*, **13,** 1065–1074.

Henjes, K., 1997: Isotropic and anisotropic correlations in turbulent wind speed data. *Bound.-Layer Meteor.,* **84,** 149–167.

Kaimal, J. C., J. C. Wyngaard, and D. A. Haugen, 1968: Deriving power spectra from a three-component sonic anemometer. *J. Appl. Meteor.*, **7,** 827–837.

——, ——, Y. Izumi, and O. R. Cote, 1972: Spectral characteristics of surface-layer turbulence. *Quart. J. Roy. Meteor. Soc.*, **98,** 563–589.

Larsen, S. E., J. B. Edson, C. W. Fairall, and P. G. Mestayer, 1993: Measurement of temperature spectra by a sonic anemometer. *J. Atmos. Oceanic Technol.*, **10,** 345–354.

Yelland, M. J., and P. K. Taylor, 1996: Wind stress measurements from the open ocean. *J. Phys. Oceanogr.*, **26,** 541–558.

——, B. I. Moat, P. K. Taylor, R. W. Pascal, J. Hutchings, and V. C. Cornell, 1998: Wind stress measurements from the open ocean corrected for airflow distortion by the ship. *J. Phys. Oceanogr.*, **28,** 1511–1526.

——, P. K. Taylor, I. E. Consterdine, and M. H. Smith, 1994: The use of the inertial dissipation technique for shipboard wind stress determination. *J. Atmos. Oceanic Technol.*, **11,** 1093–1108.

Notice to Authors: One of the following statements, whichever is appropriate, must be signed by all authors (use multiple forms if needed) of a manuscript and received by the chief editor to which the manuscript is submitted. See "AMS Authors' Guide" (*Bulletin of the AMS*, August 1995). Requests for further information should be addressed to American Meteorological Society, 45 Beacon Street, Boston, MA., 02108. (e-mail: amspubs@ametsoc.org)

AGREEMENT TO TRANSFER COPYRIGHT
(For non-U.S. Government)

Copyright to the article entitled_____

_____

by_____
assigned and transferred exclusively to the American Meteorological Society (hereinafter referred to as AMS) effective

if and when the article is accepted for publication in_____
or in any other AMS journal in which the article may be published with the authors' consent. The authors, however, reserve 1) all proprietary rights other than copyright, such as patent rights, and 2) the right to use all or part of this article in future lectures, press releases, and reviews of their own. Certain additional reproduction rights are granted by sections 107 and 108 of the U.S. Copyright Law. All other uses will be subject to the limitations given in the copyright statement of the AMS journal in which the article is published. To be signed by all authors or if the manuscript is a "work made for hire," by the employer, who is the "legal author" under the U.S. Copyright Law.

Signature	Signature
Print name	Print name
Title if signed by employer	Title if signed by employer
Date	Date
Signature	Signature
Print name	Print name
Title if signed by employer	Title if signed by employer
Date	Date

Note: The form below is to be used for a work of the U.S. Government for which copyright protection is not available under Title 17, Section 105. A work of the U.S. Government is a work prepared by an officer or employee of the U. S. Government as part of this person's official duties.

CERTIFICATION OF U.S. GOVERNMENT MANUSCRIPT

The article entitled_____

_____

by _____
is hereby certified to be a work of the U.S. Government , to have been prepared by the author(s) as officer(s) or employee(s) of the U.S. Government as part of the author(s) official duties, and therefore to be precluded from copyright protection. It is further certified that the article has not been published previously in any language and it is agreed to promptly notify the chief editor if the manuscript is submitted for publication elsewhere before its disposition by the American Meteorological Society.

Signature	Signature
Print name	Print name
Title if signed by employer	Title if signed by employer
Date	Date
Signature	Signature
Print name	Print name
Title if signed by employer	Title if signed by employer
U.S. Government Agency	U.S. Government Agency
Date	Date